Pergamon

PII: S0191-8141(98)00010-8

Journal of Structural Geology, Vol. 20, No. 6, pp. 695 to 705, 1998

0191-8141/98 $19.00 + 0.00

The influence of three-dimensional grain size distributions on the rheology of polyphase rocks

RENÉE HEILBRONNER*

Geologisch-Paläontologisches Institut, Basel, Switzerland

and

DAVID BRUHN†

Geologisches Institut, ETH Zentrum, Zürich, Switzerland

(*Received* 6 *December* 1995; *accepted in revised form* 28 *January* 1998)

Abstract—In this study, the relation between the deformational behaviour of two-phase rocks and the grain size distributions of the constituent phases is investigated. Samples of hot isostatically pressed 50:50 volume percent mixtures of calcite and anhydrite were experimentally deformed in a triaxial apparatus at a temperature of 500°C, a confining pressure of 300 MPa, and a strain rate of 2×10^{-5} s^{-1}. For calcite and anhydrite these are the deformational conditions for dislocation and diffusion creep, respectively, and for a grain size of 8 μm these are the conditions of the equiviscous point. It was found that samples from different batches of the synthetic material, while having an identical average two-dimensional grain size, displayed significantly different rheological behaviour. The ensuing full analysis revealed that the volumetric three-dimensional grain size distributions of the different phases and the different batches varied significantly. Since the anhydrite is in the transition between the dislocation and the grain size sensitive diffusion creep regime, the deformational behaviour of the bulk depends critically on the grain size distribution of the anhydrite phase. The usefulness of the concept of an average grain size is discussed. © 1998 Elsevier Science Ltd. All rights reserved

INTRODUCTION

There are many experimental and theoretical studies to testify that grain size plays an important role in the rheology of materials. If deformation occurs by grain size sensitive flow, grain size, flow stress, temperature and strain rate are intimately related, as described by the following simplified equation.

$$\dot{\varepsilon} = A \exp(-Q/RT)\sigma^n d^{-m} \quad (1)$$

Grain size may by viewed as the result of a given stress level and a given strain rate or it may be viewed as the critical parameter which selects whether a material is going to deform by grain size sensitive diffusion creep or by grain size insensitive dislocation creep, at a given stress level and strain rate. This mutual dependence of deformation mechanism on grain size and vice versa has been demonstrated for many different rock types and metals (e.g. Schmid *et al.*, 1977; Brace and Kohlstedt, 1980; Walker *et al.*, 1990). In the diffusion creep regime, minor changes in grain size have major effects on the flow stress–strain rate relationship. Depending on the value of m [equation (1)], flow stress may decrease drastically if grain size decreases. In paleopiezometry this flow stress–grain size relation is used in so far as the grain size of dynamically recrystallized grains is regarded as a measure for the differential stress that was active during deformation (Twiss, 1977; Derby, 1990).

When considering grain size from a theoretical point of view, for example, in a flow law, grain size is defined by a diameter, d, which is understood to be the diameter of the three-dimensional (3-D) grains (e.g. Nabarro, 1948; Rutter, 1976; Rutter and Brodie, 1988; Schmid 1982; Twiss, 1977, and many others). In as much as d is a number and not a distribution function, it is implied that either the grain size distribution is monodisperse (i.e. all grains are of the same size) or that d is an average value and that the dispersion of the grain size distribution is not relevant to the deformational behaviour described by the flow law. The distribution or spread of grain size is considered only in so far as it is recognized that the large and the small grain size fractions may behave differently, in particular that—at threshold conditions—the small fractions may deform by grain size sensitive diffusion creep while the large fraction is still in the (grain size insensitive) dislocation creep regime (Ghosh and Raj, 1981; Raj and Ghosh, 1981; Hamilton, 1985; Freeman and Ferguson, 1986; Wang, 1994). From this point of view, a chemically monophase material appears as a mixture

*Please send correspondence to: Renée Heilbronner, Geologisch-Paläontologisches Institut, Bernoullistr. 32, 4056 Basel, Switzerland, E-mail: HEILBRONNER@UBACLU.UNIBAS.CH.

†Now at: Department of Geology and Geophysics, University of Minnesota, 108 Pillsbury Hall, Minneapolis MN 55455-0219, U.S.A.

of two different physical materials with different rheological properties. And each of these materials is again described by a 'typical' or average grain size.

In contrast, when grain size is obtained as the result of a measurement, it is usually a two-dimensional (2-D) measure which is derived from 2-D sections. Most commonly, a histogram of linear intercepts of cross-sectional shapes is used to calculate an average or typical grain size (for linear intercept method, see, e.g. Underwood, 1970). In order to obtain the 3-D mean grain size from the 2-D mean, most commonly, factors between 1.28 and 1.5 are used (e.g. Panozzo, 1982; Panozzo Heilbronner, 1992; Dell'Angelo and Olgaard, 1995). Calculating the 3-D mean grain size from the 2-D mean by multiplication with a constant implies that the ratio between the average of the 2-D and the 3-D grain size distribution is a constant, irrespective of the distribution of grain size. However, one is easily convinced on theoretical and empirical grounds, that this underlying assumption is wrong (e.g. Bach, 1967).

Occasionally, not only the measures of central tendency, but also the measures of dispersion, skewness and kurtosis of the 2-D grain size distributions are used to calculate the corresponding statistical descriptors of the 3-D distribution. Again, the erroneous assumption is that the relation between the statistical descriptors of the 2-D and the 3-D grain size distributions should be linear (e.g. Friedman, 1962)

Finally, it is usually neglected that the numerical density distribution (the frequency distribution) does not adequately portray the physical significance of the 3-D grain size distribution. For this purpose, the volumetric or weight distributions of grain size should be used. Moreover, for the comparison with the results of sieve analyses, it is clear that volumetric grain size distributions are more appropriate (not the number of grains per fraction but their fractional volume is of importance).

The motivation for this paper is given by a set of rock deformation experiments during which synthetic samples of anhydrite–calcite mixtures were deformed at various temperatures and strain rates (Bruhn, 1996). In several samples where the average grain size of both phases appeared to be identical, the deformational behaviour was significantly different. After verifying that the different flow stresses could not be accounted for by experimental artefacts or measuring errors, the SEM back scatter images were examined again. While the identity of the average grain size could be verified within statistical limits, it became apparent that the grain size distribution varied from anhydrite to calcite and from one type of sample preparation to the next. The need for a more discriminating analysis of grain size was obvious.

SAMPLE PREPARATION AND EXPERIMENTAL PROCEDURE

For the deformation experiments, fine-grained synthetic calcite–anhydrite aggregates were used. The starting materials were reagent grade powders of hemihydrate ($CaSO_4 \cdot 1/2\ H_2O$) and calcite ($CaCO_3$). Calcite and anhydrite were selected as end-member phases, because their rheologies and deformation microstructures were studied previously on samples made from the same starting materials (calcite: Olgaard and Dell'Angelo, 1993; anhydrite: Dell'Angelo and Olgaard, 1995).

The synthetic rocks used in the experiments were fabricated in three steps: (1) Mixing of the powders; (2) uniaxial cold-pressing of the powder mixtures; and (3) hot isostatic pressing (HIPing).

Calcite and hemihydrate powders were combined in various proportions (see Bruhn, 1996). In a first attempt, the powders were mixed as a suspension with ethanol in closed containers by rolling for 24 h. After drying and densification, the rock appeared homogeneous, however, optical and electron microscopy of the samples revealed a tendency for the anhydrites to form clusters of 10–20 grains (e.g. Fig. 1a).

To avoid clustering, large alumina balls (diameter approx. 2 cm) were added to the ethanol-powder suspension during the mixing process. The end result was that the anhydrite was not only well dispersed, but also, that the largest anhydrite grains were reduced in size (Fig. 1b). In the following, the first procedure (without alumina balls) will be called HIP-1, the second (with alumina balls) HIP-2.

After the mixing, the powders were dried on a hot plate and cold-pressed into steel canisters. To drive all the water off the hemihydrate, the mixed and cold-pressed powders were kept at 500°C for 24 h, before the canisters were welded shut and hot isostatically pressed at 550°C and a confining pressure of 200 MPa for 4 h. From the resulting synthetic rocks, cylinders were cored for triaxial deformation experiments.

RHEOLOGY OF TWO-PHASE AGGREGATES

End-members

The anhydrite end-member of this study is identical to the one described by Dell'Angelo and Olgaard (1995) and Olgaard and Dell'Angelo (1995). There, two flow regimes were recognized: (a) a twinning and dislocation creep regime at high stresses and (b) a regime of diffusion creep with grain boundary sliding at low stresses, with a slow transition of the flow law parameters and the diagnostic microstructures and textures between the regimes. In those studies, the average grain sizes were given as 8 μm and 5 μm. At high stresses (regime 1), the stress exponent, n, was found to be

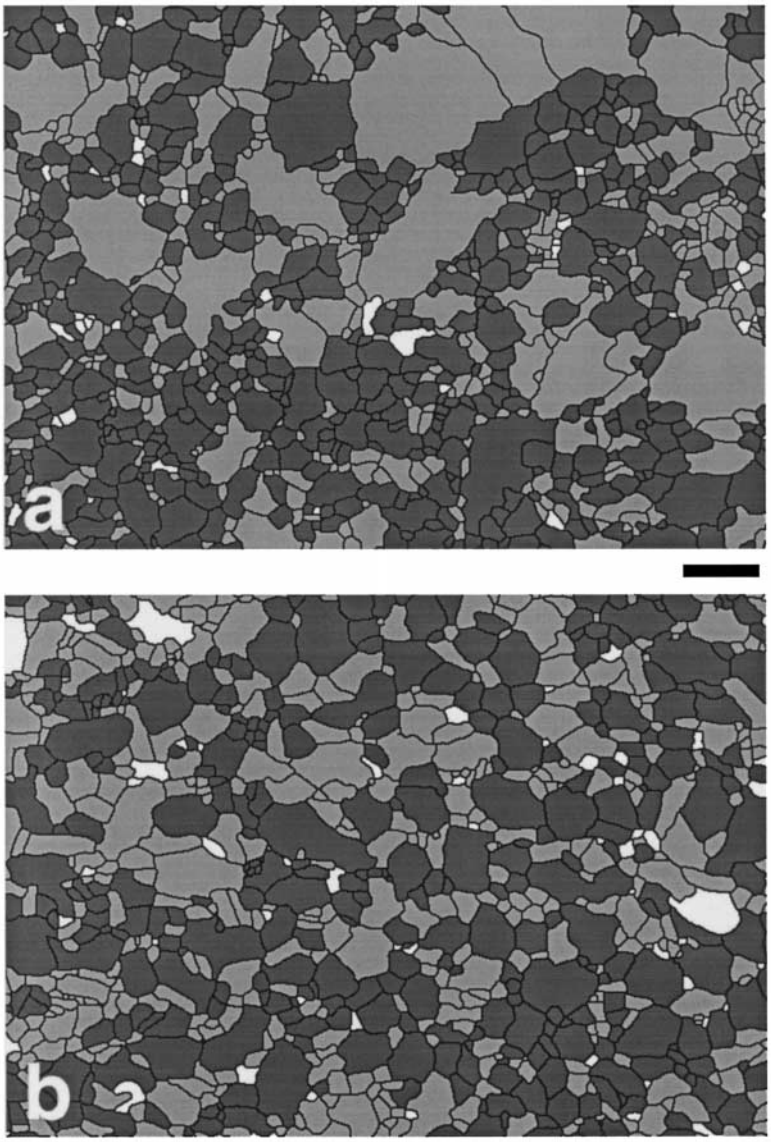

Fig. 1. Pre-processed images of SEM micrographs of 50:50 mixture of calcite and anhydrite. Light grey—anhydrite, dark grey—calcite, white—hole. (a) Sample prepared after the HIP-1 technique, (b) sample prepared after the HIP-2 technique (see text). Scale bar (10 μm) applies to both microstructures.

5; the grain size exponent, m, was 0. At low stresses (regime 2), n was found to be 1 and m was 3.

The calcite end-member of this study is the one described by Olgaard and Dell'Angelo (1993). There, the average grain size was given as approximately 8 μm. At high stresses, calcite deformed dominantly by dislocation creep with a stress exponent, n, of 4. At low stresses, the influence of diffusion creep increases, and the stress exponent n was 2.

The rheological behaviour of pure anhydrite and calcite is summarized in Fig. 2. The flow laws of pure calcite and pure anhydrite predict that at a stress level of 75 MPa, deformation of both phases occurs at the same stress. However, calcite deforms by dislocation creep while the anhydrite deformation is in transition between dislocation and diffusion creep. Due to ongoing recrystallization in the anhydrite at the experimental conditions chosen for the present study, this transition spans more than one order of magnitude of strain rate. Thus, it is possible that samples in which dislocation creep is the dominant deformation mechanism, may deform at stresses of 120 MPa (Dell'Angelo and Olgaard, 1995), while an increasing contribution of diffusion creep leads to correspondingly lower sample stresses. In other words, with anhydrite being in the grain size sensitive flow regime (with the grain size exponent, m, of 3), a small decrease in grain size should lower the strength of anhydrite significantly. The grain size of calcite does not affect its strength because it is not in the grain size sensitive regime. Provided that the weaker phase controls the behaviour of the mixed aggregates, the flow stresses of the mixtures of anhydrite and calcite should be close to that of the anhydrite if strain rates are relatively slow, and close to that of calcite if strain rates are relatively fast.

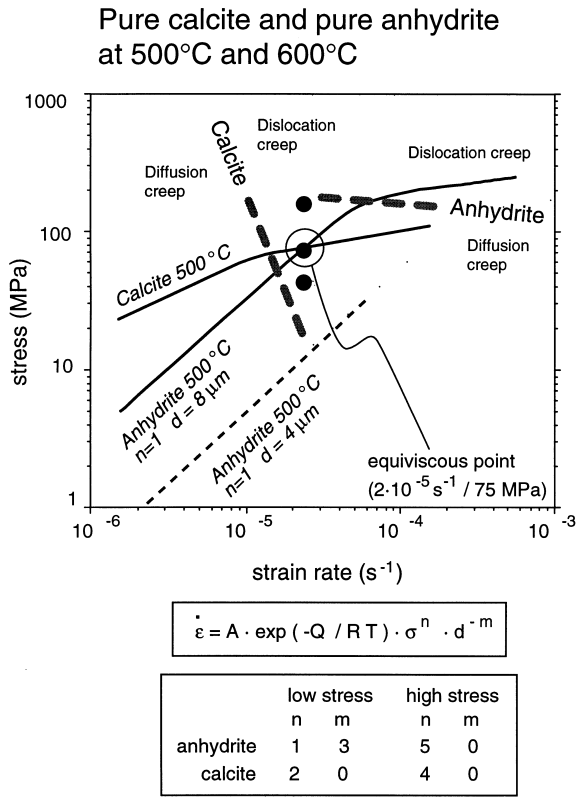

	low stress		high stress	
	n	m	n	m
anhydrite	1	3	5	0
calcite	2	0	4	0

Fig. 2. Log stress vs log strain rate diagrams for pure anhydrite and pure calcite. Black dots—experimental results for 50:50 mixtures of anhydrite and calcite (H1132.1, H1240.2, H1164.1, see Table 1). Solid lines—experimental results for 500°C (Bruhn, 1996). Stippled black line—calculated line for 4 μm grain size. Heavy grey stipples—boundary between dislocation and diffusion creep fields.

50:50 mixtures of anhydrite and calcite

In contrast to the reasoning outlined above, it was found, that on the whole, at 500°C, HIP-1 mixtures were much stronger than pure calcite and stronger than the fine-grained anhydrite in the diffusion creep regime, but similar in strength to anhydrite in the dislocation creep regime. One was weaker than both end-members. The reproducibility of the HIP-2 samples was much better than that of the HIP-1 samples. On average, they were weaker than the HIP-1 mixtures, with flow stresses plotting in between the strengths of pure calcite and anhydrite, with a tendency to be slightly closer to the weaker phase.

In this paper we will focus on five samples with 50:50 mixtures. Two are undeformed samples: H1185.1 and H1185.2 which are HIP-1 and HIP-2 mixtures, respectively. Three are experimentally deformed samples (500°C, 300 MPa, 2×10^{-5} s^{-1}): H1164.1 and H1132.1 are HIP-1 mixtures, H1240.2 is a HIP-2 mixture. The experimental results for these samples are compiled in Table 1; and shown in Fig. 2.

Table 1. Experimental results

Sample*	Mixture	Flow stress (MPa)	Total strain (%)
H1132.1	HIP-1	43	19
H1240.2	HIP-2	72	5
H1164.1	HIP-1	150	18

*Experimental conditions: Temperature = 500°C; confining pressure = 300 MPa; strain rate = 2×10^{-5} s^{-1}.

H1164.1 deformed at a flow stress which is above that of the equiviscous point, i.e. the sample is stronger than the calcite and anhydrite end-members. Sample H1240.2 deformed at the flow stress which corresponds to the equiviscous point for 8 μm grain size of anhydrite. Sample H1132.1 was weaker than calcite and weaker than anhydrite at 8 μm grain size. Since anhydrite is in the grain-size sensitive regime, the reduction of grain size from 8 to 4 μm should lower the flow stress of pure anhydrite from 75 to approx. 10 MPa. The calculated curve is shown as a black dashed line in Fig. 2.

Under the assumption that the average grain size of anhydrite is 8 μm, sample H1240.2 deforms at the correct stress level, while sample H1164.1 is too strong and sample H1132.1 is too weak. If the grain size of anhydrite is smaller than 8 μm (between 8 μm and 4 μm), sample H1132.1 may be considered to deform at the 'correct' flow stress, while the measured flow stresses of samples H1164.1 (150 MPa) and H1240.2 (72 MPa), which deform at the stress of the (stronger) calcite, appear too high.

It is obvious that the interpretation of these data points depends very critically on the correct assessment of grain size. Therefore, we will now turn to possible methods of grain size measurement and to a critical review of the results.

ANALYSIS OF 2-D GRAIN SIZE DISTRIBUTIONS BY IMAGE ANALYSIS METHODS

In order to obtain the full 2-D grain size distribution, the following analysis was performed. On transparencies which were placed over the back-scattered SEM images, the calcite and anhydrite grains were outlined. The drawings were scanned on a flat bed scanner, using a resolution of 300 dpi. The calcite and anhydrite grains were coloured with different grey levels using Adobe Photoshop™ 3.0 graphic software. Figure 1 shows pre-processed images of samples H1185.1 and H1185.2.

Using the public domain software NIH Image 1.60, the calcite and anhydrite grains where extracted by appropriate grey level slicing. Using the 'Analyze' menu, the bitmaps were evaluated, and the list of measurements (areas of cross-sectional shapes) was transferred to Kaleidagraph™ spread sheet program. The sizes of the cross sectional areas of the grains were given in pixels, and had to be scaled and converted to μm^2. Dividing the areas by π and taking the root, the radii of the equivalent circles (=circles with the same area as the cross-sectional shape) were obtained.

Table 2. List of symbols

Symbol	Explanation
area	measured area of the cross-sectional shape
r	radius of the equivalent circle
$d = 2{\cdot}r$	diameter of the equivalent circle
$f(x)$	numerical density distribution (ungrouped data) of x
$h(d)$	numerical density histogram (grouped data): number or percent (%) of diameters in given interval of d
R	radius of sphere
$D = 2{\cdot}R$	diameter of sphere
$h(D)$	numerical density histogram of diameter of spheres
$V(D)$	volumetric density histogram (grouped data): percent of volume of spheres within given interval of D
$\mu(x)$	mean of distribution of x
$s(x)$	standard deviation of distribution of x
sk(x)	skewness of distribution of x

$$d = 2 \cdot r = 2 \cdot (\text{area}/\pi)^{1/2} = 1.128 \cdot \text{area}^{1/2} \qquad (2)$$

where d = diameter, r = radius of the equivalent circle, area = measured area of the cross-sectional shape (explanation of symbols, see Table 2).

Figure 3 shows the results as histograms of the number of grains per interval of diameter, d. The mean diameters and standard deviations of these 2-D distributions were calculated; they are listed in Table 3. The mean grain size, the standard deviation and the skewness are listed, too (Table 3). The mean grain sizes of anhydrite of the HIP-1 and HIP-2 samples are exactly identical (2.3 μm); those of calcite are 2.6 and 3.1 μm, respectively. However, from a rheological point of view, i.e. since calcite does not deform in the grain size sensitive regime, the grain size of calcite is not considered important.

While the mean grain size of anhydrite is constant for both mixtures, the sorting of preparation HIP-2 is much better than that of HIP-1. This is shown by a smaller standard deviation of 1.4 vs 2.4 and a smaller skewness of 1.2 vs 3.3. Note that a large positive skewness is indicative of the presence of a few very large grains.

Obviously, these average grain sizes are much smaller than those indicated by Dell'Angelo and Olgaard (1995) and Olgaard and Dell'Angelo (1993) for the end-members, i.e. smaller than those that were assumed for the calculation of the equiviscous point (Fig. 2). In as much as the average 2-D grain size determination used here is an equivalent to the method

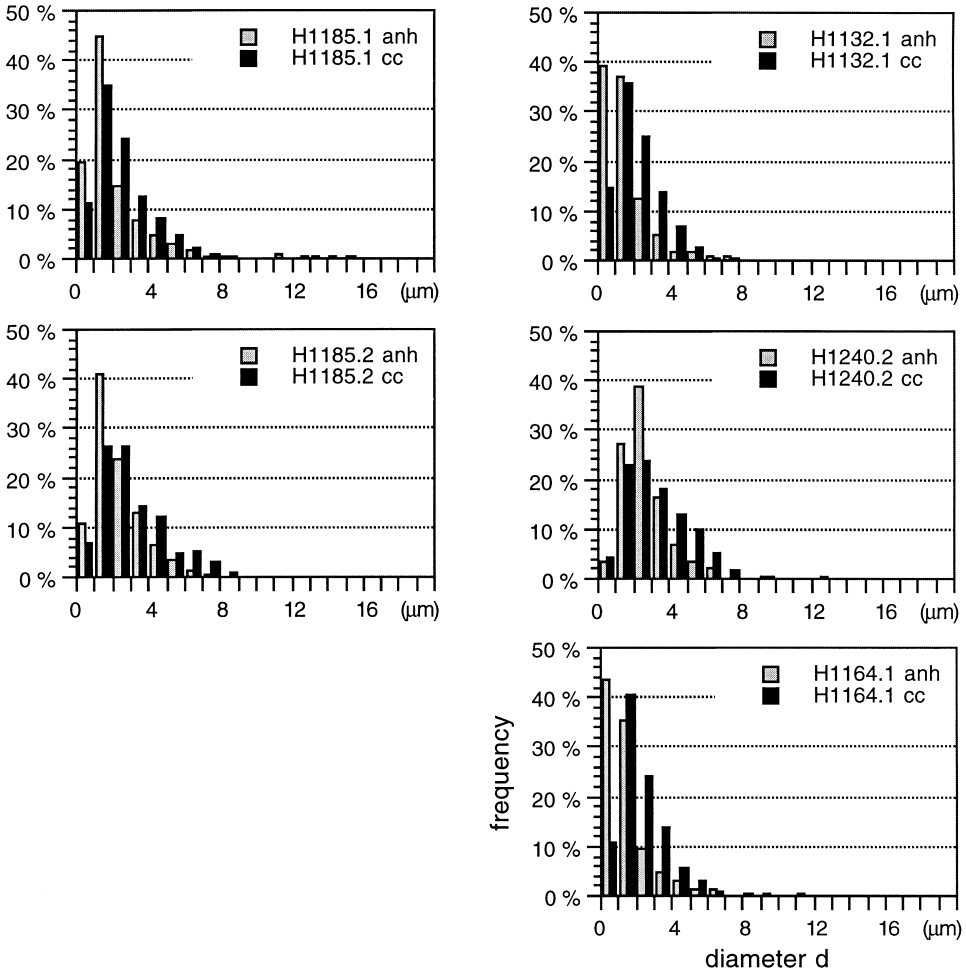

Fig. 3. Numerical density distributions, $h(d)$, of 2-D grain size. d—diameter of equivalent circle. Left column: undeformed samples, right column: deformed samples. anh—anhydrite, cc—calcite.

Table 3. Statistical descriptors of numerical density distribution of 2-D grain size

	No. of grains		$\mu(d)$* in μm		$s(d)$* in μm		sk(d)*	
Sample	anh	cc	anh	cc	anh	cc	anh	cc
H1185.1	617	833	2.3	2.6	2.4	1.7	3.3	1.7
H1185.2	545	393	2.3	3.1	1.4	1.8	1.2	1.0
H1132.1	730	593	1.6	2.3	1.4	1.4	2.2	1.2
H1240.2	437	313	2.7	3.3	1.4	1.8	1.5	1.0
H1164.1	694	430	1.6	2.3	1.7	1.4	3.3	1.5

*Statistical descriptors of numerical density histograms, $h(d)$, i.e. of grouped data; d = diameter of 2-D grains.

of average intercept length used in the above cited papers, the comparison of 'average grain size' is valid. Note that the factor between the average intercept length of 8 μm of the anhydrite end-member (as measured by Dell'Angelo and Olgaard, 1995) and the 2.5 μm 'average grain size' of anhydrite of the samples deformed here is approximately 3, and the deformation of the anhydrite by itself is expected to take place at a flow stress of approximately 2.5 MPa! In other words, compared to the extrapolations implied in Fig. 2, all samples deformed at flow stresses that were much too high. This point will be taken up later.

Interestingly enough, the deformed samples do not preserve the initial average grain size. The mean grain size of anhydrite of the HIP-1 samples (H1132.1 and H1164.1) decreases to a value of 1.6 μm, that of the HIP-2 sample (H1240.2) increases to 2.7 μm. Similarly, the mean grain size of calcite of the HIP-1 samples decreases from 2.6 to 2.3 μm, while that of the HIP-2 sample increases slightly from 3.1 to 3.3 μm. In the case of calcite, the standard deviations vary in an analogue fashion as if scaled by the same factor as the means while the skewnesses remain more or less unaltered.

From the analysis of the 2-D grain size distribution, one may conclude that on the whole, these 'increases' and 'decreases' of average grain size are not due to the deformation processes or the type of mixture; instead, that they are an expression of the inhomogeneities of the starting materials. This is clear at least in the case of calcite. In the case of anhydrite the picture is not so clear and a more detailed discussion of the preservation or destruction of the initial grain size distribution during deformation will be presented later.

Most important, however, is the observation that neither the mean nor any other statistical descriptor of the 2-D grain size distribution corresponds to the increase of flow strength from H1132.1 (43 MPa) to H1240.2 (72 MPa) to H1164.1 (150 MPa). Judging from the mean, for example (Fig. 5a), the HIP-1 mixtures, H1132.1 and H1164.1, should behave similarly while the flow stress of the HIP-2 mixture should not be intermediate but highest of the three.

Table 4. Statistical descriptors of numerical density distribution of 3-D grain size

	$\mu(D)$* in μm		$s(D)$* in μm		sk(D)*	
Sample	anh	cc	anh	cc	anh	cc
H1185.1	1.8	2.2	1.6	1.5	4.3	1.9
H1185.2	2.1	2.8	1.2	1.6	1.5	1.3
H1132.1	1.2	2.0	1.0	1.2	2.7	1.3
H1240.2	2.7	3.2	1.2	1.7	1.8	1.3
H1164.1	1.1	2.1	1.1	1.2	4.3	1.7

*Statistical descriptors of numerical density histograms, $h(D)$, i.e. grouped data; D = diameter of 3-D grains.

CALCULATION OF 3-D GRAIN SIZE DISTRIBUTIONS FROM 2-D GRAIN SIZE DISTRIBUTIONS

From the histogram, $h(d)$, of the numerical density distribution of the 2-D grain size, $f(d)$, the 3-D grain size distribution can be calculated (see Table 2 for definitions) and various methods are given in the literature (e.g. Spektor, 1950; Saltykov, 1958; Underwood, 1968). Here we will use the StripStar program (see Appendix), which when applied to a given set of input returns the same result as the Schwartz–Saltykov method (best described in Underwood, 1968). The theory underlying the StripStar program and the Schwartz–Saltykov method is the same. Using StripStar for interpreting the results in a manner as described below has a few advantages: (a) the program exists as a public domain software, (b) in addition to 3-D numerical density histograms, $h(D)$, 3-D volumetric histograms, $V(D)$, are calculated, a representation which is much more useful for physical interpretations, and (c) the possible negative occurrences in the resulting 3-D histograms (the presence of the so-called antispheres) are not neglected but used as additional information.

The statistical descriptors of the numerical density histograms, $h(D)$, of the 3-D grain size distributions are listed in Table 4. The calculated volumetric histograms of 3-D grain size, $V(D)$, are presented in Fig. 4, the statistical descriptors are listed in Table 5.

The first thing to note is that the statistical descriptors of the numerical density histograms of the 3-D grain size distributions (Table 4) are quite similar to those of the 2-D distributions (Table 3). This means that the statistical descriptors of the 3-D distribution, $h(D)$, are equally unsuited to explain the differences between the rheological behaviour of the samples as those of the 2-D distributions, $h(d)$, (see also Fig. 5b). In fact, not only the statistical parameters but the entire shape of the numerical 2-D and 3-D grain size distributions are very similar. For this reason, the $h(D)$ histograms are not shown.

The contrast between two and three dimensions is brought out if the volumetric histograms are considered. The statistical descriptors and the histograms,

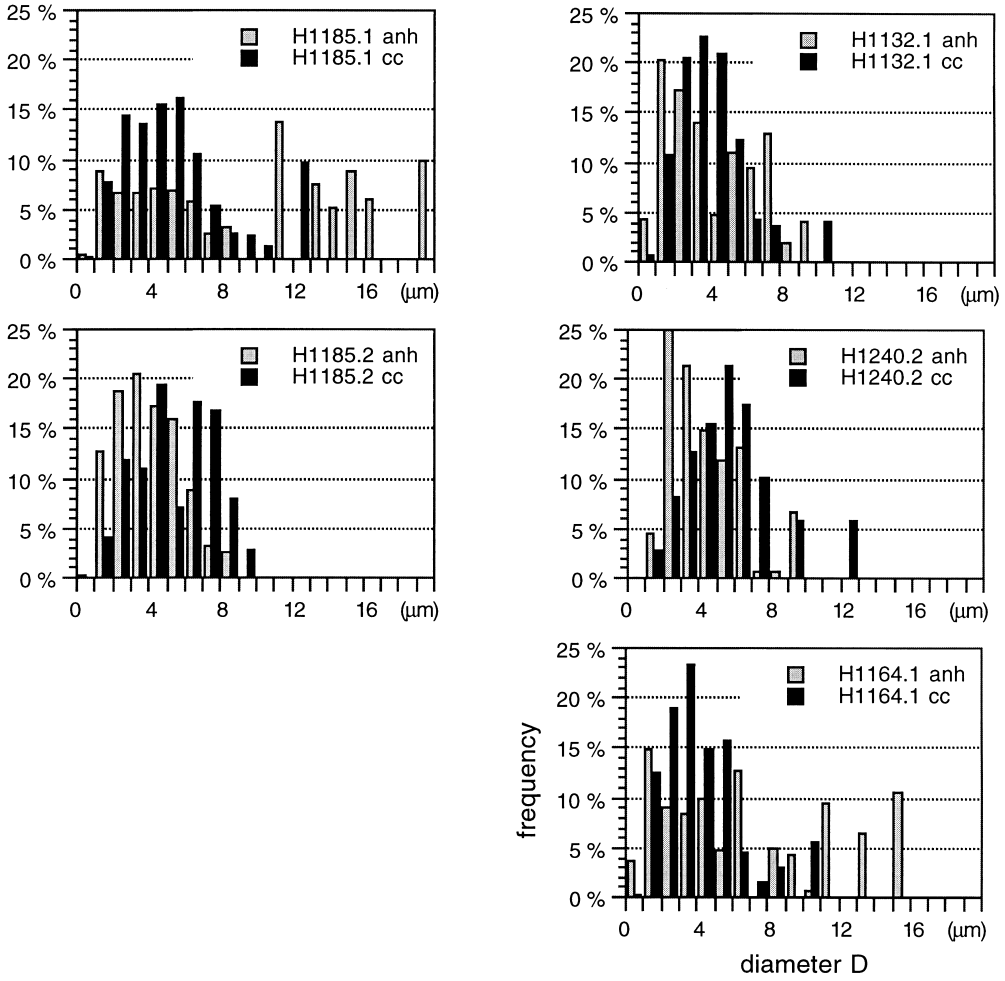

Fig. 4. Volumetric density distributions, $V(D)$, of 3-D grain size. D—diameter of sphere. Left column: undeformed samples, right column: deformed samples. anh—anhydrite, cc—calcite.

$V(D)$, of the 3-D volumetric grain size distributions are quite different (Table 5 and Fig. 4). The mean of the 3-D volumetric grain size distribution, $V(R)$, of anhydrite is smallest in H1132.1 (4.2 μm), the sample that deformed at the lowest stress, and highest in sample H1164.1 (6.8 μm), which deformed at the highest stress. For the first time, a similar trend of mean grain size and flow stress can be noted for the anhydrite, but not for calcite (Fig. 5c). This is a first indication that anhydrite, by its grain size sensitivity, may govern the rheological behaviour of the bulk rock.

Note, however, that the average values of the 3-D volumetric grain size cannot easily be compared to the average intercept lengths used for the analysis of the pure end-members (Dell'Angelo and Olgaard, 1995) since the latter are equivalent to the 2-D measure. Thus, the coincidence of the results found here with the data assembled in Fig. 2 could still be fortuitous. In fact, if the shape of the grain size distribution of the material used in the cited paper were similar to those of the synthetic materials used here, the average value of the 3-D volumetric grain size of the pure end-members would be expected to be larger. The problem of having to compare the means of published 2-D and those of newly calculated 3-D distributions has to be kept in mind for the following discussion.

DISCUSSION

If we consider the volumetric grain size distribution as a whole (Fig. 4), we note that the maximum anhydrite grain size in H1240.2 and H1132.1 is 10 μm,

Table 5. Statistical descriptors of volumetric density distribution of 3-D grain size

	$\mu(D)$* in μm		$s(D)$* in μm		sk(D)*	
Sample	anh	cc	anh	cc	anh	cc
H1185.1	9.8	5.5	5.9	3.1	0.1	1.0
H1185.2	4.1	5.4	1.8	2.1	0.4	−0.1
H1132.1	4.2	4.1	2.5	2.0	0.4	1.3
H1240.2	4.4	5.8	2.0	2.5	0.9	1.0
H1164.1	6.8	4.2	4.7	2.2	0.5	1.2

*Statistical descriptors of volumetric density histograms, $V(D)$, i.e. of grouped data; D = diameter of 3-D grains.

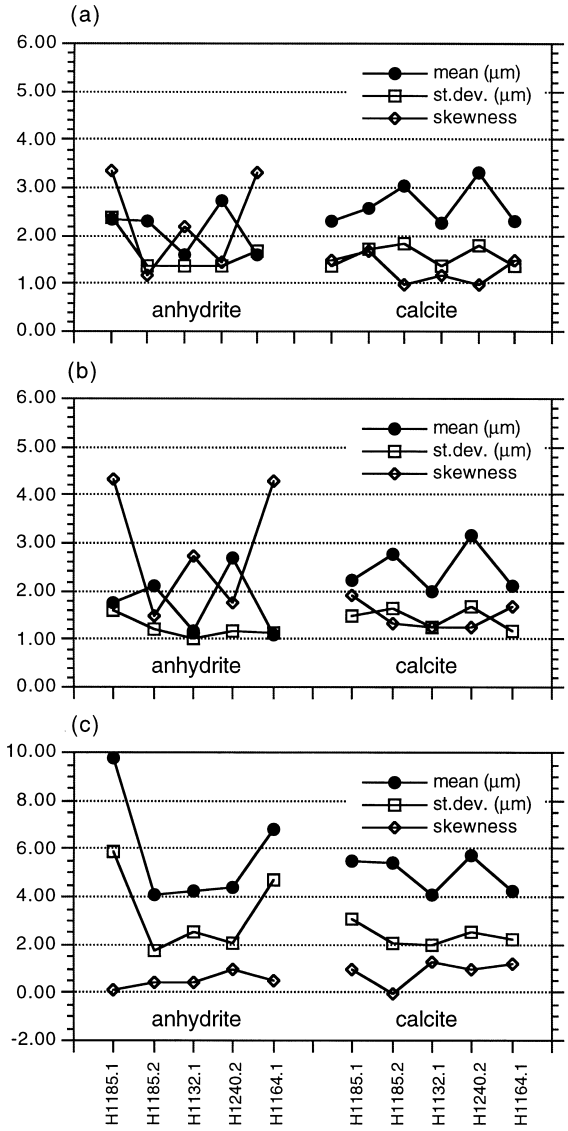

Fig. 5. Statistical parameters calculated for histograms of 2-D and 3-D grain size distributions: (a) numerical density distribution of 2-D grain size, $h(d)$, (b) numerical density distribution of 3-D grain size, $h(D)$, (c) volumetric density distribution of 3-D grain size, $V(D)$.

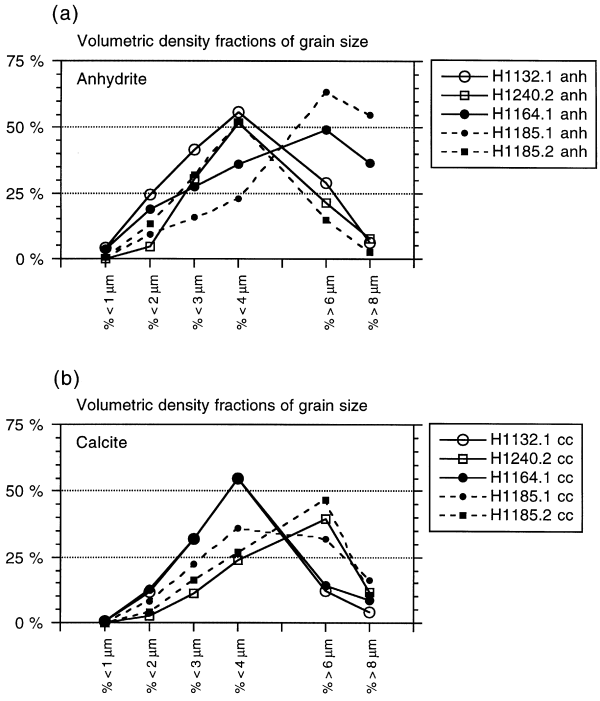

Fig. 6. Volume fractions of coarse and fine grains of 3-D grain size distributions of starting material and deformed samples: (a) for anhydrite, (b) for calcite.

while it is 16 μm in H1164.1. Various small and large fractions of the $V(D)$ grain size distributions of anhydrite and calcite are represented in Fig. 6(a & b), respectively. While the grain size distribution of calcite is unimodal and symmetric in the HIP-1 and HIP-2 samples, the anhydrite of the HIP-1 samples displays a rather spread out or even bimodal distribution. Such a distribution appears to be 'unnatural'—an artefact of the production process—and without having measured it, it is assumed that the grain size distribution of the (natural) end-member is more closely approximated by the improved HIP-2 material.

The anhydrite phase of the HIP-1 starting material (H1185.1) has a large fraction of relatively large grains: 70% of the volume (of anhydrite) consists of grains whose diameter is larger than 6 μm, only 25% of the volume consists of grains that are smaller than 4 μm (Fig. 6a). In contrast, 50 vol.% of the anhydrite of the HIP-2 starting material (H1185.2) consists of grains that are smaller than 4 μm, only 15 vol.% consist of grains which are larger than 6 μm. After the experiments, the volume fraction of large anhydrite grains of the HIP-1 mixture is reduced (H1164.1) while that of the HIP-2 mixture (H1240.2) remains more or less unaltered. Judging from Fig. 6(a), sample H1132.1 looks much more like a HIP-2 than HIP-1 mixture. The only way this can be explained is by considering the inhomogeneity of the HIP-1 batch which yields samples whose grain size statistic may vary much more than those of the HIP-2 batch.

With respect to the grain size distribution of the calcite phase, the HIP-1 and HIP-2 starting materials do not differ as much (Fig. 6b) as with respect to the anhydrite. Thirty-five percent of the calcite volume of HIP-1 and 25% of the HIP-2 batch consist of grains that are smaller than 4 μm, while 35% and 45%, respectively, are grains larger than 6 μm. In each case, approximately 30 vol.% of the calcite consist of grains which have a diameter from 4 to 6 μm. The calcite grain size distribution of the deformed HIP-2 sample (H1240.2) is not altered significantly while the deformed HIP-1 samples (H1164.1 and H1132.1) show a slight tendency for grain size reduction: 50 vol.% of the deformed calcite consists of grains that are smaller than 4 μm as opposed to 35 vol.% of the undeformed sample (H1185.1). At the same time, less than 15 vol.% of the deformed calcite consists of grains larger than 6 μm as opposed to more than 30% in the

undeformed sample. After the experiment, again approximately 35% of the volume of calcite consists of grains that are between 4 and 6 μm in diameter.

The weakest sample (H1132.1) has the largest fraction of small anhydrite grains, more than 50 vol.% are below 4 μm. The strongest sample (H1164.1) has the smallest fraction of small anhydrite grains, only 35 vol.% are below 4 μm. The strongest sample also has the largest fraction of large grains: 50 vol.% are above 6 μm, 35 vol.% are above 8 μm; while the weaker samples only have 25 vol.% of grains larger than 6 μm and less than 10 vol.% above 8 μm. The main difference among the two weaker samples, H1132.1 and H1240.2, lies within the very smallest fractions. The weakest sample, H1132.1, consists of 25 vol.% of grains that are smaller than 2 μm, while the intermediate sample, H1240.2, has less than 5 vol.% of these small grains.

Note that the experimental data of the pure endmembers refer to a grain size of 8 μm (Fig. 2). If we consider anhydrite in the range above 4 μm, approximately 75 vol.% of the HIP-1 and 50 vol.% of the HIP-2 starting material fall within this range, and thus, can be expected to deform at the stress level shown in Fig. 2. Only 25 or 50 vol.% of the anhydrite has a smaller grain size, and thus, are expected to deform at lower stress levels. We also note that 65 and 75 vol.% of the calcite of HIP-1 and HIP-2 respectively are in the grain size range above 4 μm, 35 and 25% below it. However, as has been mentioned, the grain size of calcite is rheologically unimportant.

Judging from the flow law one would expect anhydrite to be the weaker phase, and thus that it should control the strength of the sample. However, two aspects have to be considered. Firstly, only a relatively small fraction of the anhydrite phase has a grain size that is significantly smaller than 5 μm. The starting material of HIP-1 and HIP-2 have from 10 to 15 vol.% of anhydrite which is smaller than 2 μm, i.e. only 5–7.5 vol.% of the total rock is expected to deform at stresses that are significantly below the equiviscous point. Secondly, since the fine-grained anhydrite does not deform by crystal plasticity, the weak grains do not elongate and hence show no tendency to form an interconnected weak layer. Note however, that the total strains are less than 20% and deformation may not have reached a steady state (as it could in a torsion rig, see Olgaard *et al.*, 1997). In other words, even the very weak fractions of anhydrite tend to remain disconnected ('inert') within the framework of the stronger anhydrite and calcite fractions. In the presence of large amounts of large grains (H1164.1), the very small grain size fraction appears to be of no importance; only in the absence of large fractions (as in H1240.2 and H1132.1), the sample with the larger fraction of very small grains flows more readily.

SUMMARY

A number of synthetic rock samples consisting of a 50:50 mixture of anhydrite and calcite were deformed at the equiviscous point calculated for aggregates of an average 2-D grain size of 8 μm. At this condition, the flow stress should be 75 MPa. However, in three identical runs, three samples of the synthetic material deformed at 43, 72 and 150 MPa. Neither the 2-D nor the 3-D numerical density distributions were capable of explaining the rheological differences. Only the consideration of the 3-D volumetric density distribution, $V(D)$ and its statistical descriptors permits a reasonable explanation of the strength differences of the samples presented in this paper.

The analysis of the deformational behaviour of the anhydrite–calcite mixtures presented in this paper is by no means exhaustive: The material that was used is quite inhomogeneous, and the experimental data base is very small. Nevertheless, we found indications that the increasing flow stress of the mixtures correlates (1) with an increasing volume fraction of large anhydrite grains (>6 μm) which are in the dislocation creep field, and (2) with a decreasing volume fraction of very small anhydrite grains (<2 μm) which are in the diffusion creep field.

At the same time, it does not appear to correlate with any aspect of the grain size distribution of the calcite. Without the formation of an interconnected weak layer, the potential of the weak phase to induce bulk deformation at low flow stresses remains 'ineffective'. It was further found that the deformation at or near the equiviscous point of calcite and anhydrite tends to preserve the grain size distribution of calcite but not that of anhydrite. The question remains if there is a threshold grain size or a threshold volume fraction of the anhydrite which may induce the aggregate to switch from dislocation to diffusion creep.

Table 6 summarizes the procedural steps that were undertaken for the determination of the 2-D and 3-D grain size distributions of the samples as discussed in this paper.

Table 6. Steps for grain size analysis by digital image analysis

1	Scanning electron microscopy of thin sections
2	Manual outlining of (bright) anhydrite and (darker) calcite grains on SEM back scatter images
3	Scanning of contoured SEM micrograph using a flatbed scanner
4	Digital pre-processing and colour coding of the phases
5	Segmentation by grey level slicing using public domain image analysis software, 'NIH Image', conversion to bitmaps which represent the cross sectional areas of anhydrite and calcite grains
6	Digital image analysis of cross-sectional areas, exporting list of results (>500 measurements per phase)
7	Calculation of equivalent diameter of cross-sectional areas using a spread sheet computer program, calculation of 2-D numerical density histogram, $h(d)$
8	Calculation of 3-D distributions, $h(D)$ and $V(D)$, from the 2-D distribution, $h(d)$, using public domain software 'StripStar'
9	Calculations of statistical descriptors of $h(D)$ and $V(D)$

CONCLUSIONS

Image analysis of several samples of two-phase synthetic rocks, deformed and undeformed, demonstrates that differences in the mean grain size, whether 2-D or 3-D, are not sufficient to account for different rheological behaviour and for differences in the flow stress. The concept of a single value for grain size, a 'typical grain size', is of very limited use and may even result in misleading interpretations. This observation could have consequences in all fields of tectonic modelling and in applications where grain size is known to play an important role; not only in grain size sensitive flow, but also in paleopiezometry, or in the interpretation of grain populations formed by the crystallization of phases from a melt, etc. It has been shown (e.g. Freeman and Ferguson, 1986) that two or more deformation mechanisms may contribute significantly to the deformation over a wide range of temperature and stress/strain rate conditions. Changes in grain size distribution may lead to changes in the bulk rheology, even if the mean grain size of the bulk rock or of the individual phases does not change. This has to be kept in mind because extrapolations of laboratory data and tectonic models are often performed for one mechanism and one grain size only.

The 3-D grain size distribution may be a critical parameter for many physical processes that take place in rocks. In order to derive it, we must measure the full 2-D numerical density distribution, $h(d)$, (not only the average intercept length) and calculate the 3-D volumetric distribution, $V(D)$, from it. It is useless to speculate on a linear relationship between the statistical descriptors of the 2-D and the 3-D grain size distributions, since we may find that the 'standard' log-normal distribution is not as ubiquitous as we have been induced to believe by looking at 2-D distributions which indeed all have a tendency to look alike. Whether 3-D grain size distributions are 'typically' unimodal–normal, log-normal (as in the case of sediments), skewed, or bimodal (as in the case of mixing powders), depends on the different physical processes (sedimentation, nucleation, grain growth, etc.) which have produced these rocks.

Acknowledgements—Support by Swiss National Science Foundation NF2000-049562.96/1 is gratefully acknowledged. Two anonymous reviewers and Peter Wanten are thanked for many valuable suggestions and corrections.

REFERENCES

Bach, G. (1967) Kugelgrössenverteilung und Verteilung der Schnittkreise. In *Proceedings of the Second International Congress for Stereology*, ed. H. Elias. Springer, New York.

Brace, W. F. and Kohlstedt, D. L. (1980) Limits on lithospheric stress imposed by laboratory experiments. *Journal of Geophysical Research* **85,** 6248–6252.

Bruhn, D. (1996) Rheology of fine-grained two-phase rocks with phases of similar strength—an experimental investigation. Unpublished PhD-thesis, ETH Zürich, Switzerland.

Dell'Angelo, L. N. and Olgaard, D. L. (1995) Experimental deformation of fine grained anhydrite: Evidence for dislocation and diffusion creep. *Journal of Geophysical Research* **100[B8],** 425–440.

Derby, B. (1990) Dynamic recrystallization and grain size. In *Deformation processes in minerals, ceramics and rocks*, eds D. J. Barber and P. G. Meredith, pp. 354–364. Unwin Hyman, London.

Freeman, B. and Ferguson, C. C. (1986) Deformation mechanism maps and micromechanics of rocks with distributed grain sizes. *Journal of Geophysical Research* **91,** 3849–3860.

Friedman, G. M. (1962) Comparison of moment measures for sieving and thin section data in sedimentary petrological studies. *Journal of Sedimentary Petrology* **32,** 15–25.

Ghosh, A. K. and Raj, R. (1981) Grain size distribution effects in superplasticity. *Acta metallurgica* **29,** 607–616.

Hamilton, C. H. (1985) Superplasticity in titanium alloys, in *Superplastic Forming. Proceedings of a Symposium on Superplastic Forming, Los Angeles-California, March 22, 1984*. American Society for Metals, Metals Park, Ohio, pp. 13–22.

Nabarro, F. R. N. (1948) Deformation of crystals by the motion of single ions: report of a conference on the strength of solids. *Proceedings of the Physical Society of London,* 75–90.

Olgaard, D. L. and Dell'Angelo, L. N. (1993) Another flow law for calcite rocks: Reagent $CaCO_3$ powders densified by HIPing. *TERRA abstracts, Abstract supplement No. 1 to TERRA nova* **5,** 294.

Olgaard, D. L. and Dell'Angelo, L. N. (1995) Grain size sensitive flow in anhydrite: Implications for deformation within evaporite decollement horizons. *EUG VIII, 9–13 April 1995*, p. 47. Strasbourg, France.

Olgaard, D. L., Stretton, I. C., Paterson, M. S., Pieri, M. and Kunze, K. (1997) The influence of high strain on rheology and microstructure: results from high temperature torsion experiments. *Proceedings of Deformation Mechanisms in Nature and Experiment*. Basel, p. 21.

Panozzo, R. (1982) Determination of size distributions of spheres from size distributions of circular sections by Monte Carlo methods. *Microscopica Acta* **86,** 37–48.

Panozzo Heilbronner, R. (1992) The autocorrelation function: an image processing tool for fabric analysis. *Tectonophysics* **212,** 351–370.

Raj, R. and Ghosh, A. K. (1981) Micromechanical modeling of creep using distributed parameters. *Acta metallurgica* **29,** 283–292.

Rutter, E. H. (1976) The kinetics of rock deformation by pressure solution. *Philosophical Transactions of the Royal Society of London A* **283,** 203–219.

Rutter, E. H. and Brodie, K. H. (1988) The role of tectonic grain size reduction in the rheological stratification of the lithosphere. *Geologische Rundschau* **77,** 295–308.

Saltykov, S. A. (1958) *Stereometric metallography*. Metallurgizdat, Moscow.

Schmid, S. M., Boland, J. N. and Paterson, M. S. (1977) Superplastic flow in fine-grained limestone. *Tectonophysics* **43,** 257–291.

Schmid, S. M. (1982) Microfabric studies as indicators of deformation mechanisms and flow laws operative in mountain building. In *Mountain building processes*, ed. K. J. Hsü, pp. 95–110. Academic Press, London.

Spektor, A. G. (1950) Distribution analysis of spherical particles in nontransparent structures. *Zavodskaya Laboratoriya*. **16,** 193.

Twiss, R. J. (1977) Theory and applicability of a recrystallized grain size paleopiezometer. In *Stress in the Earth*, ed. M. Wyss, pp. 227–244. Birkhäuser, Basel.

Underwood, E. E. (1968) Particle size distribution. In *Quantitative microscopy*, eds R. T. DeHoff and F. N. Rhines, p. 149. MacGraw-Hill, New York.

Underwood, E. E. (1970) *Quantitative Stereology*. Addison Wesley, Reading, Mass., p. 274.

Walker, A. N., Rutter, E. H. and Brodie, K. H. (1990) Experimental study of grain-size sensitive flow of synthetic, hot-pressed calcite rocks. *Geological Society of London Special Publication* **54,** 259–282.

Wang, J. N. (1994) The effect of grain size distribution on the rheological behavior of polycrystalline materials. *Journal of Structural Geology* **16,** 961–970.

APPENDIX

The computer program described below is designed to calculate the distribution of radii of spheres, $h(R)$, from the distribution of the radii of cross-sectional circles, $h(r)$. While any (positive) distribution $h(R)$ may be the generator of a distribution $h(r)$, the reverse is not true. As an example: every positive distribution $h(R)$ generates a distribution $h(r)$ that trails off to zero. Therefore, a distribution $h(r)$ whose lower classes are empty cannot possibly be generated from any positive $h(R)$.

The computer program StripStar calculates a distribution $h(R)$ irrespective of the input distribution, $h(r)$. If a given distribution $h(r)$ is a valid distribution of sectional circles, the result of the calculations of StripStar will be the generator distribution $h(R)$ which consists of positive occurrences only. If, however, $h(r)$ is an invalid distribution, the resulting distribution $h(R)$ will feature negative occurrences, i.e. antispheres. The meaning of antispheres is to mathematically account for empty classes in the histogram of sections, and to 'annihilate' surplus sectional circles in the classes below an empty class. In practice, one will strive to prepare (i.e. measure) a distribution $h(r)$ which has no empty classes and which produces the least number of antispheres. Means for obtaining good $h(r)$ distributions are adjusting the class width and/or increasing the sample size.

The underlying concept of StripStar is simple. The measured size distribution of sectional circles, $h(r)$, is compared to one that would be obtained if the size distribution of spheres, $h(R)$, was the uniform distribution. This 'ideal' size distribution will be denoted $h(r)_u$. The theoretical values of the 'ideal' $h(r_i)_u$ are calculated by the following equations:

$$p_{ij} = \left[(R_j^2 - r_{(i-1)}^2)^{1/2} - (R_j^2 - r_i^2)^{1/2}\right] / R_{\max}\, pc \qquad \text{(A1)}$$

$$p_i = \sum_{j=1}^{k} \left[(R_j^2 - r_{(i-1)}^2)^{1/2} - (R_j^2 - r_i^2)^{1/2}\right] / R_{\max} qno \qquad \text{(A2)}$$

where:

p_{ij} = probability to obtain sections of size r_i from sphere of size R_j
p_i = probability to obtain sections of size $r_i = h(r_i)_u$
$R_{\max}$ = radius of the largest sphere
R_j = radius of a sphere
r_i = radius of a sectional circle
k = number of classes of R and r

The measured distribution $h(r)$ is worked off ('stripped off') from the largest to the smallest class. The largest size class of spheres is at the same time the largest possible class of sectional circles:

$$r_{\max} = R_{\max} \qquad \text{(A3)}$$

Starting at the largest value of $h(r)$, a unit starting proportion of spheres is created with a radius $R_k = R_{\max}$. The size distribution of sectional circles, $h(r)_k$, pertaining to this largest class of spheres is calculated and 'stripped' from the measured (total) distribution $h(r)$. As a result, the remaining $h(r)$ is zero for $r = r_k$. The remaining $h(r)$, in particular the remainder of $h(r)$ in the next lower class, $h(r_{k-1})$, is analysed next. The value $h(r_{k-1})$ is divided by the theoretical value of the 'ideal' $h(r)_u$ at this point and a proportional fraction of R_{k-1} is set aside. Again, the size distribution pertaining to the proportion of R_{k-1} is stripped off the remaining $h(r)$.

By repeating this procedure down to the last, i.e. smallest size class, the entire distribution $h(r)$ is stripped to zero, i.e. $h(r) = 0.00$ for all grain sizes. In the course of successively stripping the distribution $h(r)$ off the individual contributions, $h(r)_i$, some classes of the remaining values $h(r)$ may drop below zero, and therefore, negative frequencies may occur. In this case, for a given i, $h(R_i)$ is calculated by comparing the absolute value of $h(d_i)$ with the 'ideal' $h(d_i)_u$, and then set to the equivalent negative value.